Journal of Inorganic and General Chemistry
ZAAC
Zeitschrift für anorganische und allgemeine Chemie
www.zaac.wiley-vch.de
ARTICLE

DOI: 10.1002/zaac.201500569

Transition Metal Complexes Containing C_2-Symmetric Bis(imidazolin-2-imine) Ligands Derived from a 1-Alkyl-3-arylimidazolin-2-ylidene

Thomas Glöge,[a] Frouke Aal,[a] Sabina-Alexandra Filimon,[b][‡] Peter G. Jones,[a] Janna Michaelis de Vasconcellos,[b] Sonja Herres-Pawlis,[c] and Matthias Tamm[a]

Dedicated to Professor F. Ekkehardt Hahn ("Ekki") on the Occasion of His 60th Birthday

Keywords: *N*-heterocyclic carbenes; N-donor ligands; Guanidines; Transition metals; Lactide polymerization

Abstract. The new *N*-heterocyclic carbene 1-(2,6-diisopropylphenyl)-3,4,5-trimethylimidazolin-2-ylidene (IPrMe) (**3**) was prepared in three steps from methyl isothiocyanate and 2,6-diisopropylaniline, affording *N*-methyl-*N*′-2,6-diisopropylthiourea (**1**). Reaction of **1** with 3-hydroxybutanone gave the imidazolin-2-thione (IPrMe)S (**2**), which was reduced with elemental potassium to the carbene IPrMe (**3**). Treatment of **3** with trimethylsilyl azide (Me_3SiN_3) in boiling toluene, followed by desilylation in methanol, gave the imidazolin-2-imine (IPrMe)NH (**4**). The ethylene-bridged diimine ligand *N*,*N*′-bis[1-(2,6-diisopropylphenyl)-3,4,5-trimethylimidazolin-2-ylidene]-1,2-ethanediamine, (IPrMe)NCH_2CH_2N(IPrMe) (**5**) was prepared by reaction of **4** with 1,2-ethyleneditosylate and subsequent deprotonation with KO*t*Bu. The reaction of **5** with metal dichlorides furnished the tetrahedral complexes [(**5**)MCl_2] [*M* = Fe (**6**), *M* = Ni (**7**), *M* = Zn (**8**)] and the square-planar complex [(**5**)$PdCl_2$] (**9**), as revealed by X-ray diffraction analyses. The X-ray crystal structures of **2**, **3**, and **4** were also established. Complex **8** and related zinc(II) bis(imidazolin-2-imine) complexes were tested in the polymerization of D,L-lactide.

Introduction

Bis(imidazolin-2-imine) ligands such as BL^{Me} and BL^{iPr},[1] and related guanidine-type ligands,[2] have found widespread use in organometallic and coordination chemistry,[3] in particular as ancillary ligands in homogeneous catalysis.[4] Because the imidazole moiety can efficiently stabilize a positive charge,[5] these diimine species are highly basic and can serve as strong N-donor ligands towards transition metals. The resulting strong polarization of the exocyclic C=N bond can be described by the two limiting resonance structures **A** and **B** for the ligands $BL^{R,R'}$ (Scheme 1), with the contribution of the dipolar mesomeric form increasing significantly upon coordination to transition metal complex fragments. As a conse-

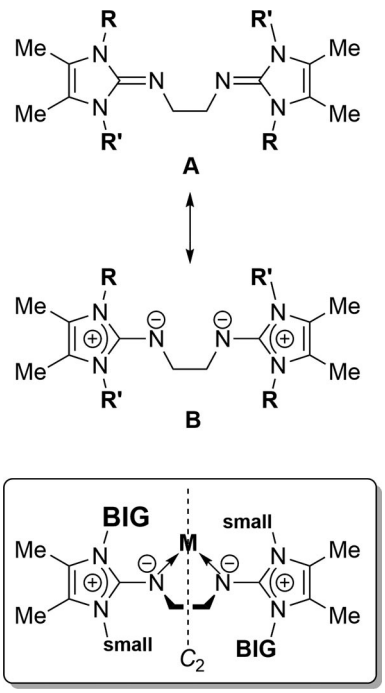

Scheme 1. Mesomeric structures (**A**, **B**) for bis(imidazolin-2-imine) ligands $BL^{R,R'}$ (BL^{Me}: *R* = *R*′ = Me; BL^{iPr}: *R* = *R*′ = *i*Pr; $BL^{Dipp,Me}$: *R* = 2,6-diisopropylphenyl, *R*′ = Me); schematic presentation of C_2-symmetric bis(imidazolin-2-imine) metal complexes (box).

* Prof. Dr. M. Tamm
Fax: +49-251-391-5309
E-Mail: m.tamm@tu-bs.de
née Börner
[a] Institut für Anorganische und Analytische Chemie
Technische Universität Braunschweig
Hagenring 30
38106 Braunschweig, Germany
[b] Institut für Anorganische Chemie
Department Chemie
Universität Paderborn
Warburger Str. 100
33098 Paderborn, Germany
[c] Lehrstuhl für Bioanorganische Chemie
Institut für Anorganische Chemie
RWTH Aachen University
Landoltweg 1
52074 Aachen, Germany
[‡] née Börner.
Supporting information for this article is available on the WWW under **http://dx.doi.org/10.1002/zaac.201500569** or from the author.

Dedicated Cluster

© 2015 WILEY-VCH Verlag GmbH & Co. KGaA, Weinheim

quence of this charge separation, the imidazole rings in the resulting metal complexes usually adopt a perpendicular orientation relative to the N–*M*–N plane, precluding any significant π-interaction with the metal-bound nitrogen atoms.

Accordingly, bis(imidazolin-2-imine) ligands with a symmetric *N*,*N*′-substitution pattern (*R* = *R*′), such as BL^{Me} and BL^{iPr}, usually form C_s- or C_{2v}-symmetric chelate complexes with four magnetically equivalent nitrogen substituents.[1] The introduction of unsymmetric imidazolin-2-ylidene moieties with nitrogen substituents of distinctly different size, however, might afford $BL^{R,R'}$ ligands (*R* = BIG ≠ *R*′ = small) that are able to form chiral C_2-symmetric complexes by adopting a conformationally stable *anti*-orientation of the *R* and *R*′ pairs of substituents as illustrated in Scheme 1 (box). In principle, this would allow the synthesis of chiral complexes for applications in asymmetric catalysis such as transfer hydrogenation.[4c,4f,4g] A similar concept was developed for related α-diimine ligands and their respective nickel(II) and palladium(II) complexes, which serve as catalysts for the production of highly branched polyethylene.[6]

To test this hypothesis, we report herein the preparation of the bis(imidazolin-2-imine) ligand $BL^{Dipp,Me}$ (**5**), which contains large 2,6-diisopropylphenyl (Dipp) and small methyl (Me) substituents, and its reaction with the metal dihalides $FeCl_2$, $NiCl_2$, $ZnCl_2$, and $PdCl_2$. This affords complexes of the type $[(BL^{Dipp,Me})MCl_2]$, which were structurally characterized to elucidate whether chiral C_2-symmetric complexes are formed.

Results and Discussion

Ligand Synthesis

Following the established synthetic route for imidazolin-2-imines,[5] an unsymmetrical N-heterocyclic carbene (NHC)[7] with one large and one small nitrogen substituent was required. We chose to synthesize the unknown 1-(2,6-diisopropylphenyl)-3,4,5-trimethylimidazolin-2-ylidene (IPrMe) (**3**). Metal complexes of a related NHC, 1-(2,6-diisopropylphenyl)-3-methylimidazolin-2-ylidene, with hydrogen atoms in the 4,5-positions have been reported and were generally prepared from the corresponding imidazolium salts without isolation of the free carbene.[8]

The preparation of the required carbene **3** commences with the reaction between methyl isothiocyanate and 2,6-diisopropylaniline, which afforded thiourea **1** according to a modified literature procedure.[9] Treatment of **1** with 3-hydroxybutanone in 1-hexanol gave the imidazolin-2-thione **2** in satisfactory yield (65 %, Scheme 2).[10] The molecular structure of **2** was established by X-ray diffraction analysis, after suitable single crystals had been obtained by diffusion of *n*-hexane into a saturated THF solution (Figure 1). As expected, the phenyl plane of the Dipp substituent adopts a perpendicular orientation relative to the imidazole ring with an interplanar angle of 88.9°, so that the molecule possesses approximate mirror symmetry (r.m.s. deviation 0.14 Å). The C–S bond length of 1.6801(12) Å falls in the range that has been established for similar compounds.[11]

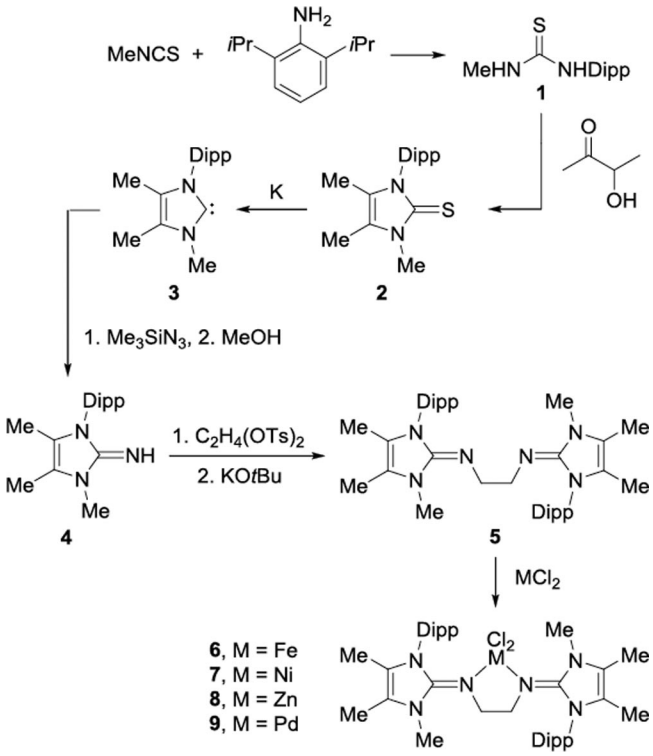

Scheme 2. Preparation of bis(imidazolin-2-imine) complexes.

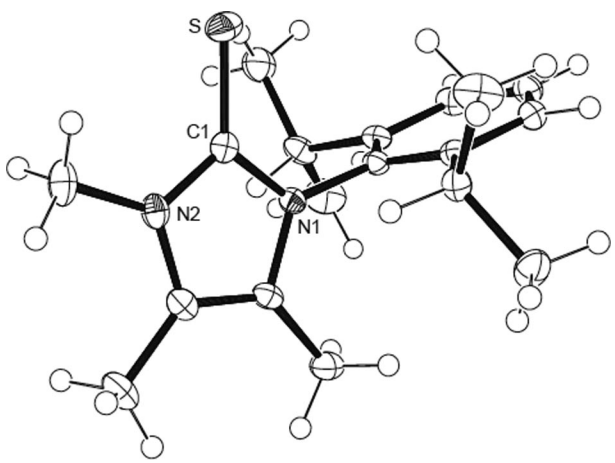

Figure 1. ORTEP diagram of **2** with thermal displacement parameters drawn at 50 % probability. Selected bond lengths /Å and angles /°: C1–S 1.6801(12), C1–N1 1.369(15), C1–N2 1.3582(15); N1–C1–N2 105.15(10).

Reduction of thione **2** proceeded by treatment with potassium metal in refluxing THF, furnishing the free *Arduengo*-type carbene **3** in satisfactory yield (79 %) as a pale yellow solid after sublimation (Scheme 2).[10] The carbene carbon atom gives rise to a characteristic low-field ^{13}C NMR signal at δ = 215.3 ppm. Single crystals suitable for X-ray diffraction analysis were obtained by cooling a saturated *n*-hexane solution of **3** to –35 °C. The resulting molecular structure represents one of only few available structures of asymmetrically

Dedicated Cluster

© 2015 WILEY-VCH Verlag GmbH & Co. KGaA, Weinheim

substituted N-heterocyclic carbenes.[12] It consists of two independent but similar molecules differing in the orientation of one isopropyl group; one molecule is shown in Figure 2. The C1–N1 and C1–N2 bond lengths of 1.3690(13) and 1.3617(13) Å and the N1–C1–N2 angle of 101.66(8)° are in good agreement with the structural parameters found for other carbenes of the imidazolin-2-ylidene-type.[13]

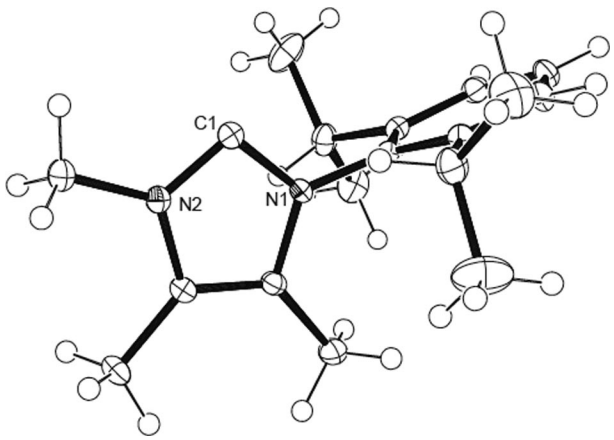

Figure 2. ORTEP diagram of one of the two crystallographically independent molecules **3** with thermal displacement parameters drawn at 50% probability. Selected bond lengths /Å and angles /°: C1–N1 1.3690(13), C1–N2 1.3617(13); N1–C1–N2 101.66(8).

The carbene **3** can be treated with trimethylsilyl azide to undergo a Staudinger type[14] reaction, and subsequent dissolution and stirring of the intermediate 2-(trimethylsilylimino)-imidazoline in methanol yields the imidazolin-2-imine **4** as a white solid (Scheme 2).[5] An X-ray diffraction analysis of **4** was performed on single crystals grown by diffusion of *n*-hexane into a saturated THF solution, and the molecular structure is shown in Figure 3. Compounds **2** and **4** are isotypic; accordingly, the latter also displays approximate mirror symmetry (r.m.s.d. 0.17 Å). The structural parameters are in excellent agreement with those established for related 1,3-dialkyl- and 1,3-diarylimidazolin-2-imines.[5] Accordingly, a relatively long

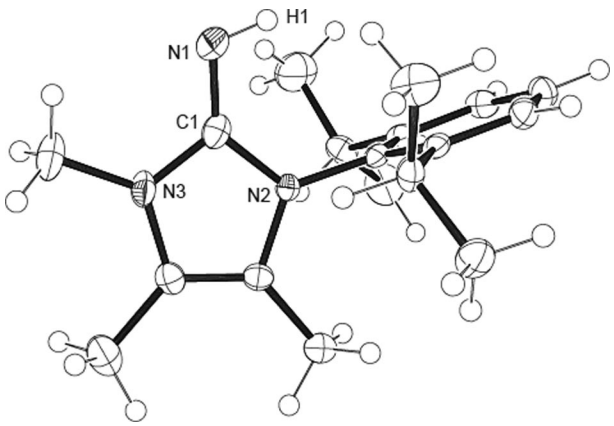

Figure 3. ORTEP diagram of imine **4** with thermal displacement parameters drawn at 50% probability. Selected bond lengths /Å and angles /°: C1–N1 1.295(2), C1–N2 1.369(2), C1–N3 1.387(2); N2–C1–N3 104.54(13).

C1–N1 bond length of 1.295(2) Å is observed that exceeds the value of about 1.28 Å expected for a typical C(sp^2)–N(sp^2) bond length.[15] Likewise, surprisingly long internal C–N distances of 1.369(2) Å (C1–N2) and 1.387(2) Å (C1–N3) are observed together with a C2–N1–C3 angle of 104.54(12)°, which lies between the values reported for imidazolium ions and imidazolin-2-ylidenes, respectively.[13] These structural parameters confirm that, from a structural point of view, electron delocalization within the heterocycle does not play an important role for such imine systems.[5] Investigation of the crystal packing of **4** reveals an intermolecular C–H···N contact of 2.64 Å, which falls below the van der Waals cut-off criterion of 2.75 Å[16] and involves the imine nitrogen atom N1 and one of the Dipp methyl groups, affording parallel zigzag chains of the molecules **4** in the solid state.

The preparation of the diimine $BL^{Dipp,Me}$ (**5**) requires the linkage of two imine molecules **4** via an ethylene bridge, which can be accomplished by the reaction of 1,2-ethylenditosylate with two equivalents of **4** followed by deprotonation with KO*t*Bu (Scheme 2). Single crystals suitable for X-ray diffraction analysis were obtained by cooling a saturated *n*-hexane solution to –25 °C. The asymmetric unit of **5** contains two independent molecules with very similar structural parameters, and therefore, only the structure of the first independent molecule is further discussed (Figure 4). It exhibits exocyclic C–N bonds of 1.2770(19) Å (C3–N1) and 1.2788(18) Å (C21–N4), which are considerably shorter than the corresponding bond in the free imine **4** [1.2947(17) Å], whereas the internal C–N bonds are elongated. These structural features indicate that charge separation and electron delocalization is even less pronounced in **5** and that its solid-state structure is well presented by the resonance structure **A** depicted in Scheme 1 (vide supra). As a measure of these effects, the parameter $\rho = 2a/(b + c)$ has been introduced for guanidine systems,[17] with *a*, *b*, and *c* representing the *exo*- (*a*) and endocyclic (*b*, *c*) C–N dis-

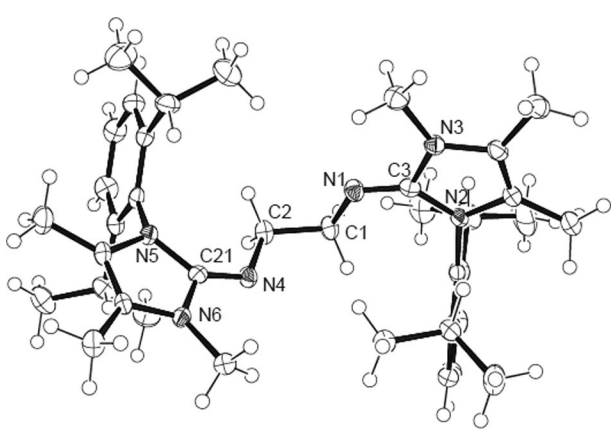

Figure 4. ORTEP diagram of one of the two crystallographically independent molecules of $BL^{Dipp,Me}$ (**5**) with thermal displacement parameters drawn at 50% probability. Selected bond lengths /Å and angles /° of the first independent molecule: C1–N1 1.4579(18), C3–N1 1.2770(19), C3–N2 1.4021(18), C3–N3 1.3855(18), C2–N4 1.4541(19), C21–N4 1.2788(18), C21–N5 1.4027(17), C21–N6 1.3849(19); N2–C3–N3 103.75(13), N5–C21–N6 104.15(12); ρ(C3) = 0.916, ρ(C21) = 0.917 (see footnote in Table 1 for a definition).

Dedicated Cluster

 © 2015 WILEY-VCH Verlag GmbH & Co. KGaA, Weinheim

tances within the CN_3 moieties. For **5**, ρ values of 0.916 and 0.917 well below unity are calculated for the two imidazolin-2-imine sites and will be used for illustration of structural changes upon metal coordination by comparison with the ρ values in $BL^{Dipp,Me}$ transition metal complexes (vide infra).

Transition Metal Complexes

The complexes $[(BL^{Dipp,Me})MCl_2]$ [*M* = Fe (**6**), *M* = Ni (**7**), *M* = Zn (**8**)] were prepared by the reaction of the diimine ligand **5** with $[FeCl_2(THF)_{1.5}]$, $[NiCl_2(DME)]$ (DME = 1,2-dimethoxyethane) or $ZnCl_2$, respectively (Scheme 2). For all three complexes, the composition was confirmed by elemental analysis and mass spectrometry. Since the complexes **6** and **7** are paramagnetic, only the diamagnetic zinc complex **8** was additionally characterized by NMR spectroscopy. It should be noted that the ^1H and ^{13}C NMR spectra do not provide evidence for the formation of a conformationally stable C_2-symmetric complex in solution, and only one set of resonances is observed for the isopropyl groups, namely one septet and two doublet ^1H NMR resonances for the tertiary CH and for the diastereotopic CH_3 groups, respectively. Single crystals for X-ray diffraction analysis were grown by diffusion of *n*-hexane into saturated solutions of **6** and **7** or by diffusion of diethyl ether into a solution of **8** in CH_2Cl_2. All complexes incorporate solvent upon crystallization, and the molecular structures of the $[(BL^{Dipp,Me})MCl_2]$ complexes in the solvates **6**·THF, **7**·1.5THF and **8**·CH_2Cl_2 are shown in Figure 5, Figure 6, and Figure 7. The nickel complex contains two independent molecules in the asymmetric unit; despite some differences in ring orientations, these are generally similar, and therefore only the structural parameters of the first independent molecule are further discussed. Pertinent structural data of complexes **6**, **7**, and **8** are assembled in Table 1.

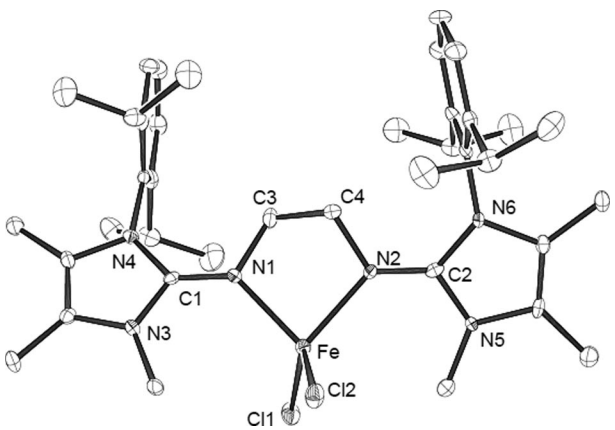

Figure 5. ORTEP diagram of $[(BL^{Dipp,Me})FeCl_2]$ (**6**) in **6**·THF with thermal displacement parameters drawn at 50 % probability.

In all complexes, the metal atoms are four-coordinate and display distorted tetrahedral arrangements with the diimine ligand forming a five-membered chelate ring with acute N1–*M*–N2 bite angles of about 86°. Similarly to the structures of related complexes of the type $[(BL^{iPr})MCl_2]$,[3e] the relative orientation of the planes containing the MCl_2 and MN_2 coordination spheres deviates significantly from the perpendicular alignment that would be expected for a regular tetrahedron; complexes **6**–**8** display dihedral angles of 79.0°, 73.3°, and 78.1°, respectively, with the nickel complex showing the largest deviation. Another method for describing the distortion from ideal arrangements in four-coordinate was proposed by *Houser*,[18] who introduced the geometry index $\tau_4 = [360° - (\alpha + \beta)]/141°$, where α and β represent the largest angles in the four-coordinate species. The values of τ_4 will range from 1.0 for a perfect tetrahedron to zero for a perfect square-planar arrangement. Intermediate structures, including trigonal-pyramidal and seesaw, will afford values $0 < \tau_4 < 1.0$. In our series **6**–**8**, the N–*M*–Cl angles are the largest (Table 1), and the calculated τ_4 values of 0.86 (**6**), 0.77 (**7**), and 0.82 (**8**) are similar to those established for $[(BL^{iPr})MCl_2]$, where a greater distortion was also observed for the corresponding nickel complex in comparison with its iron and zinc congeners.[3e]

The metal-nitrogen and metal-chlorine distances are also similar to those established for the corresponding $[(BL^{iPr})MCl_2]$ complexes (*M* = Fe, Ni, Zn)[3e,4d] and for related bis(guanidine) iron, nickel, and zinc complexes.[19] As expected, the ρ values increase upon metal coordination from

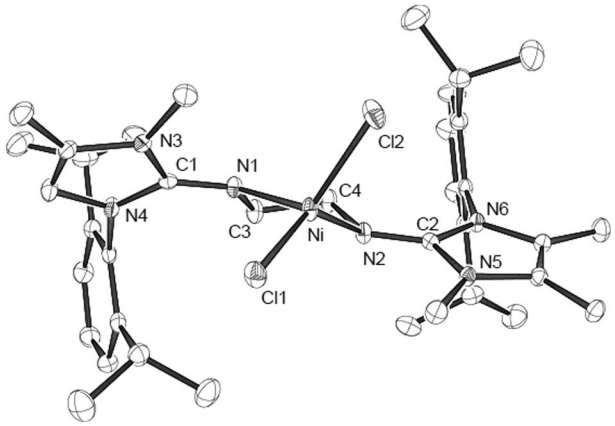

Figure 6. ORTEP diagram of $[(BL^{Dipp,Me})NiCl_2]$ (**7**) in **7**·1.5THF with thermal displacement parameters drawn at 50 % probability.

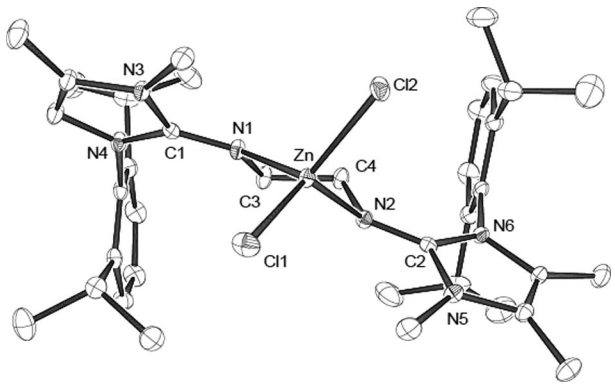

Figure 7. ORTEP diagram of $[(BL^{Dipp,Me})ZnCl_2]$ (**8**) in **8**·CH_2Cl_2 with thermal displacement parameters drawn at 50 % probability.

Dedicated Cluster

© 2015 WILEY-VCH Verlag GmbH & Co. KGaA, Weinheim

Table 1. Selected bond lengths /Å and angles /° in metal complexes **6**–**9**.

	6·THF	**7**·1½THF[e)]	**8**·CH_2Cl_2	**9**·CH_3CN
M–N1	2.0660(17)	1.9885(11)	2.0286(9)	2.0455(11)
M–N2	2.0816(18)	2.0006(11)	2.0418(9)	2.0307(11)
M–Cl1	2.2911(7)	2.2477(4)	2.2402(3)	2.3231(3)
M–Cl2	2.2934(6)	2.2624(4)	2.2586(3)	2.3090(3)
C3–N1	1.317(3)	1.3202(17)	1.3170(14)	1.3243(16)
C3–N3	1.369(3)	1.3653(17)	1.3595(14)	1.3573(16)
C3–N4	1.400(3)	1.3704(17)	1.3796(13)	1.3673(16)
C21–N2	1.325(3)	1.3220(17)	1.3183(14)	1.3245(16)
C21–N5	1.368(3)	1.3696(17)	1.3684(13)	1.3544(16)
C21–N6	1.381(3)	1.3714(17)	1.3758(13)	1.3714(15)
N1–*M*–N2	85.74(5)	85.65(5)	86.51(4)	80.03(4)
Cl1–*M*–Cl2	117.38(2)	111.63(2)	110.26(1)	90.40(1)
N1–*M*–Cl1	105.03(5)	116.36(4)	109.02(3)	95.70(3)
N1–*M*–Cl2	118.54(6)	105.01(3)	118.97(3)	173.04(3)
N2–*M*–Cl1	120.42(6)	100.95(3)	125.51(3)	173.71(3)
N2–*M*–Cl2	106.21(5)	135.39(3)	105.64(3)	93.61(3)
MCl_2/MN_2[a)]	79.0	73.3	78.1	5.5
M–N–C–N	22.6, 21.5	45.8, 40.5	35.1, 46.5	–59.2, 44.9
τ_4[b)]	0.86	0.77	0.82	0.09
Imidazole[c)]	41.4	63.2	63.0	3.3
ρ[d)]	0.951, 0.964	0.965, 0.965	0.962, 0.961	0.972, 0.972

a) Angle between MCl_2 and MN_2 planes. b) $\tau_4 = [360°– (\alpha + \beta)]/141$, where α and β represent the largest angles in four-coordinate species. c) Angle between imidazole planes. d) $\rho = 2a/(b + c)$, with *a*, *b* and *c* representing the *exo*- (*a*) and endocyclic (*b*, *c*) distances within the CN_3 guanidine moiety. e) Values for one of the two crystallographically independent molecules.

0.916 and 0.917 in the free $BL^{Dipp,Me}$ ligand to ca. 0.95–0.97 (Table 1), indicating a substantial charge delocalization, albeit to a smaller extent than found for half-sandwich cyclopentadienyl and arene ruthenium complexes, where significantly stronger metal–nitrogen interaction is observed.[3a,4c,4g] Indeed, the ligands adopt the anticipated C_2-symmetric conformation shown in Scheme 1 (box); however, the *M*–N–C–N torsion angles are comparatively small and range from 21.5° in **6** to 46.5° in **8**, thus deviating substantially from a perpendicular orientation of the imidazole rings relative to the MN_2 planes. The methyl substituents point towards the MCl_2 moiety, and inspection of the structures reveals that only a small barrier can be expected for the interconversion between the enantiomeric C_2-symmetric conformations. This is corroborated by the NMR spectra of the zinc complex **8**, which reveal averaged C_{2v} symmetry in solution on the NMR time scale (vide supra). Noteworthy, the dichloromethane solvent molecule of **8** is well-ordered and its hydrogen atoms each make one C–H···Cl contact to a chlorine atom of the $ZnCl_2$ group.

Since the complexes **6**–**8** display distorted tetrahedral arrangements, the preparation of the square-planar complex of the $BL^{Dipp,Me}$ ligand was attempted, which might afford a higher barrier because of a coplanar orientation of the MN_2 and MCl_2 planes. Accordingly, $BL^{Dipp,Me}$ (**5**) was treated with [(COD)$PdCl_2$] (COD = 1,4-cyclooctadiene) in THF, which afforded the complex [$(BL^{Dipp,Me})PdCl_2$] (**9**) in almost quantitative yield as a red crystalline solid. The ^{1}H NMR spectrum exhibits broad signals for the isopropyl CH_3 and CH and also for the NCH_3 hydrogen atoms, indicating that rotation around the exocyclic $N–C_{imidazole}$ bonds is slow at room temperature on the NMR time-scale. Single crystals for X-ray diffraction analysis were isolated from acetonitrile solution at –34 °C; the resulting molecular structure (Figure 8) confirms the expected square-planar coordination sphere around the palladium atom ($\tau_4 = 0.09$). The Pd–N and Pd–Cl bond lengths are similar to those established for other bis(imidazolin-2-imine) palladium(II) chloride complexes,[20] e.g. [$(BL^{iPr})PdCl_2$] (Table 1).[3f] However, the complex displays C_s rather than the expected C_2 symmetry (r.m.s.d. 0.01 Å), with the methyl and Dipp N-substituents each pointing to the same side of the square-planar PdN_2Cl_2 moiety. The acetonitrile molecule is well-ordered, and its hydrogen atoms (all clearly located) form C–H···Cl contacts to the $PdCl_2$ group.

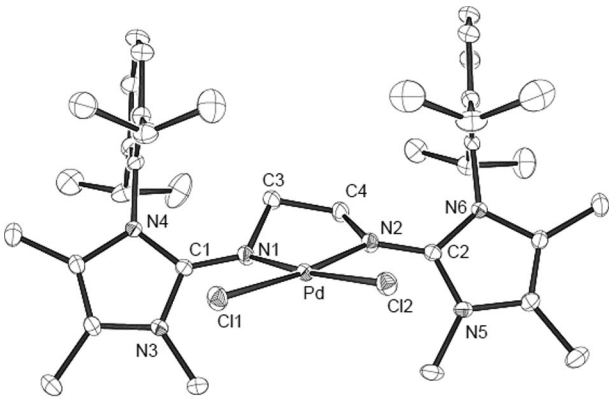

Figure 8. ORTEP diagram of [$(BL^{Dipp,Me})PdCl_2$] (**9**) in **9**·CH_3CN with thermal displacement parameters drawn at 50 % probability.

Since the observed line broadening in the ^{1}H NMR spectrum of **9** gave evidence for a fluxional process, we performed a temperature-dependent NMR study (see the Supporting Information). Below –50 °C, separate signals indicate the presence of two isomers in a 1:2.3 ratio, each giving rise to three singlets for the methyl CH_3 groups together with two septets and

Dedicated Cluster

 © 2015 WILEY-VCH Verlag GmbH & Co. KGaA, Weinheim

four doublets for the isopropyl CH_3 and CH groups, respectively. We tentatively assign these resonances to C_s- and C_2-symmetric conformers, suggesting that interconversion between chiral C_2-symmetric enantiomers can be indeed slowed down at low temperature, but that their energy is (too) close to that of the achiral C_s-symmetric conformer.

For comparison and for the catalytic study described below, the zinc(II) chloride complex **10** containing the pincer ligand 2,6-bis[(1,3-di-*tert*-butylimidazolin-2-imino)methyl]pyridine (TL^{tBu})[21] was prepared in high yield by reaction of TL^{tBu} with anhydrous $ZnCl_2$ in THF (Scheme 3). Elemental analysis confirmed the general formula [(TL^{tBu})$ZnCl_2$]. Single-crystals of **10**, suitable for X-ray diffraction analysis, were obtained from THF/*n*-hexane solution. The molecular structure in Figure 9 reveals a bidentate κ^2 coordination mode of the ligand through the pyridine nitrogen atom N2 and the imidazolin-2-imine nitrogen atom N1, with one imdiazolin-2-imine moiety remaining uncoordinated. This resembles the situation found for related cobalt(II) and iron(II) complexes of the type [(TL^{tBu}-κN^1:κN^2)MCl_2] (*M* = Co, Fe).[21c] The zinc atom resides in a distorted tetrahedral environment (τ_4 = 0.87), with the Zn–$N1_{imine}$ bond [1.982(3) Å] being shorter than the Zn–$N2_{pyridine}$ bond (2.088(3) Å], which can be explained by the stronger electron donating capability of the guanidine in comparison with the pyridine ligand. However, the symmetry of the ^{1}H NMR spectrum in [D_6]acetone indicates fast exchange between the coordinated and uncoordinated imidazolin-2-imine arms in solution at room temperature, potentially by a five-coordinate transition state.

Crystallization of **10** from dichloromethane/*n*-pentane solution gave single crystals of **10**·HCl·CH_2Cl_2, in which the uncoordinated imine moiety has reacted with traces of hydrogen chloride from the chlorinated solvent (Figure 10). The zinc coordination sphere is similar to that in **10**, whereas protonation at nitrogen atom N3 affords a considerably longer exocyclic C19–N3 bond, shorter endocyclic C19–N6 and C19–N7 bonds and consequently an increase of the ρ value from 0.92 in **10** to 1.02 in **10**·HCl (Table 2). The chloride counterion is involved in a short contact N3–H03···Cl3, whose dimensions Cl3–H03 2.32 Å and N3–H03–Cl3 167° indicate a strong hydrogen bond.[22]

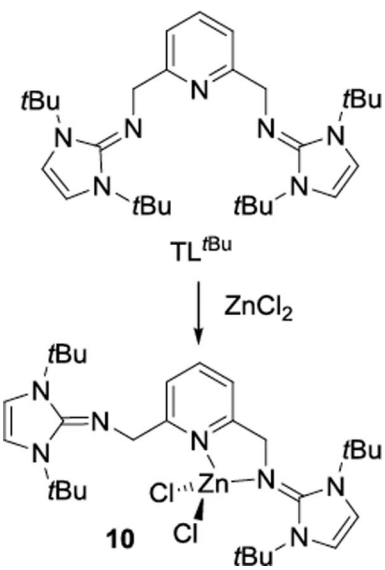

Scheme 3. Preparation of [(TL^{tBu}-κN^1:κN^2)$ZnCl_2$] (**10**).

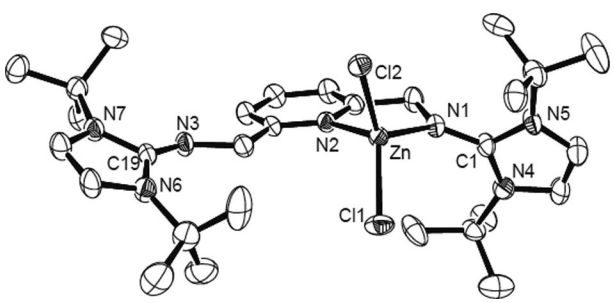

Figure 9. ORTEP diagram of [(TL^{tBu})$ZnCl_2$] (**10**) in **10**·THF with thermal displacement parameters drawn at 50% probability.

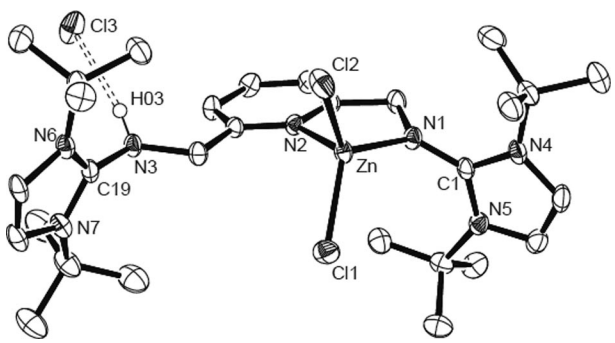

Figure 10. ORTEP diagram of **10**·HCl in **10**·HCl·CH_2Cl_2 with thermal displacement parameters drawn at 50% probability.

Table 2. Selected bond lengths /Å and angles /° in **10**·THF and **10**·HCl·CH_2Cl_2.

	10·THF	**10**·HCl·CH_2Cl_2
Zn–N1	1.982(3)	1.966(2)
Zn–N2	2.088(3)	2.091(2)
Zn–Cl1	2.2391(10)	2.2320(8)
Zn–Cl2	2.2543(9)	2.2363(8)
C1–N1	1.341(4)	1.343(3)
C1–N4	1.365(4)	1.372(3)
C1–N5	1.382(4)	1.376(4)
C19–N3	1.293(4)	1.379(3)
C19–N6	1.407(4)	1.360(4)
C19–N7	1.400(4)	1.356(3)
N1–Zn–N2	83.23(11)	82.67(9)
Cl1–Zn–Cl2	113.18(4)	110.27(3)
N1–Zn–Cl1	113.33(9)	116.20(7)
N1–Zn–Cl2	119.98(9)	121.43(7)
N2–Zn–Cl1	118.37(8)	114.17(6)
N2–Zn–Cl2	105.42(8)	108.95(7)
MCl_2/MN_2[a)]	81.7	85.7
Zn–N1–C1–N5	82.6	84.8
τ_4[b)]	0.86	0.87
ρ[c)]	0.97, 0.92	0.98, 1.02

a) Angle between MCl_2 and MN_2 planes. b) $\tau_4 = [360° - (\alpha + \beta)]/141$, where α and β represent the largest angles in four-coordinate species. c) $\rho = 2a/(b + c)$, with *a*, *b* and *c* representing the *exo*- (*a*) and endocyclic (*b*, *c*) distances within the CN_3 guanidine moiety.

Dedicated Cluster

© 2015 WILEY-VCH Verlag GmbH & Co. KGaA, Weinheim

Lactide Polymerization

It has been demonstrated that guanidine zinc complexes serve as efficient catalysts for the ring-opening polymerization of D,L-lactide,[4d,17b,19b,23] and in comparison with conventional alkoxide or alkylzinc complexes,[24] these systems offer the advantage of high stability towards air and moisture. In addition, the (potential) C_2 symmetry of the complex [(BL^{Dipp,Me})ZnCl$_2$] (**8**) might have an impact on the tacticity of the resulting polylactide (PLA) material. Therefore, the performance of this complex in the bulk polymerization of D,L-lactide was studied and compared to the performance of the related complexes [(TL^{tBu})ZnCl$_2$] (**10**), [(BL^{Me})ZnCl$_2$] (**11**),[4d] and [(BL^{iPr})ZnCl$_2$] (**12**)[3e] (Figure 11). Accordingly, the initiator and D,L-lactide (ratio 1:500, 0.2 mol-%) were heated at 150 °C. After reaction times of 24 h or 48 h, the melt was dissolved in dichloromethane, and then the PLA was precipitated in cold ethanol, isolated, and dried in a vacuum at 50 °C. In order to rate the catalytic activity of the complexes, the polymer yield was determined and the molecular weights and the polydispersity of the isolated PLA material was established by gel permeation chromatography (Table 3). For two runs with catalysts **8** and **11**, the tacticity and the probability of heterotactic enchainment (P_r) was analyzed by homonuclear decoupled ^{1}H NMR spectroscopy.[25]

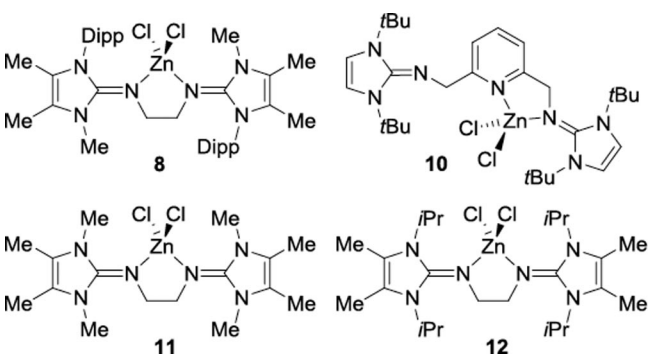

Figure 11. Bis(imidazolin-2-imine) zinc(II) chloride complexes as initiators for lactide polymerization.

Table 3. Polymerization of D,L-lactide with **8**, **9**, **11**, and **12**.[a)]

Initiator	Time /h	Yield /%	M_w /g·mol^{-1}	PD[b)]	P_r[c)]
8	24	88	48,800	1.9	0.52
8	48	90	38,000	1.9	–
10	48	16	20,300	1.6	–
11[d)]	24	85	50,700	2.0	0.53
11[d)]	48	89	54,800	1.9	–
12	24	79	36,300	2.0	–
12	48	82	36,600	1.8	–

a) Reaction conditions: initiator (0.2 mol %), 150 °C. b) PD = M_w/M_n where M_n is the number average molar mass. c) From analysis of the ^{1}H homonuclear decoupled NMR spectrum using the equation P_r = [sis]^2/2. d) Values taken from Ref. [4d].

All complexes containing bidentate bis(imidazolin-2-imine) ligands gave high PLA yields (ca. 80 %–90 %) with comparatively narrow polydispersities (around 2.0) and molecular weights ranging between 36,000 and 50,000 g·mol^{-1}. In contrast, complex **10** afforded PLA in poor yield, indicating that the TL^{tBu} ligand does not represent a suitable ancillary ligand for the development of Zn^{II} lactide polymerization catalysts. Determination of similar P_r values of ca. 0.5 for the complexes [(BL^{Dipp,Me})ZnCl$_2$] (**8**) [(BL^{Me})ZnCl$_2$] (**11**)[4d] reveals that the stereochemistry of the resulting polymer is not influenced by the presence of the potentially C_2-symmetric ligand in **8**.[25] Similar results were reported for aluminum complexes with bidentate N-donor ligands, which induced only slight enhancement for isotactic enchainment despite C_2 symmetry in the crystal structures.[26]

Conclusions

The bis(imidazolin-2-imine) ligand (IPrMe)NCH$_2$CH$_2$N-(IPrMe) (BL^{Dipp,Me}) (**5**) was prepared via the new N-heterocyclic carbene IPrMe with an asymmetric *N*,*N*′-substitution pattern. BL^{Dipp,Me} forms transition metal complexes [(BL^{Dipp,Me})*M*Cl$_2$] (*M* = Fe, Ni, Co, Pd). The tetrahedral iron, nickel, and zinc complexes exhibit, as expected, C_2-symmetric conformation in the solid state. In contrast, a C_s-symmetric orientation is found for the square-planar palladium complex, with the Dipp and Me groups each pointing to the same side of the PdN$_2$Cl$_2$ coordination sphere. NMR studies reveal fast interconversion between the C_2- and C_s-symmetric conformers in solution, and the use of these ligands in asymmetric homogeneous catalysis therefore seems to be less promising, as confirmed by use of the zinc complex [(BL^{Dipp,Me})*M*Cl$_2$] as an initiator for the polymerization of D,L-lactide. Nevertheless, coordination to other complex fragments with larger ancillary ligands and the potential to form stronger metal–nitrogen bonds might afford C_2-symmetric complexes of higher conformational stability. This could be expected for half-sandwich cyclopentadienyl and arene ruthenium complexes of the type [(η^5-Cp)Ru(BL^{Dipp,Me})]$^+$ and [(η^5-arene)Ru(BL^{Dipp,Me})]$^{2+}$.[3a,4c,4g] In addition, the use of chiral counterions in these systems would also facilitate chiral resolution, which is essential for the use of such complexes in asymmetric hydrogen transfer catalysis.[4f]

Experimental Section

General: All operations were performed in an atmosphere of dry argon by using Schlenk and vacuum techniques. All solvents were purified by standard methods and distilled prior to use. ^{1}H and ^{13}C NMR spectra were recorded at room temperature (ca. 298 K) with Bruker DPX 200 and Bruker DPX 400 devices; chemical shifts are reported in ppm relative to TMS. The spin coupling patterns are indicated as s (singlet), d (doublet), m (multiplet), sept (septet) and br (broad, for unresolved signals); *o* (*ortho*), *m* (*meta*), *p* (*para*), and *i* (*ipso*) indicate the position of carbon atoms aromatic substituents. Elemental analyses (C, H, N) were performed with a Vario EL III CHNS elemental analyzer. Mass spectrometry was performed with a Finnigan MAT 90 device. Methyl isothiocyanate, 2,6-diisopropylaniline, 3-hydroxybutanone, [Ni(DME)Cl$_2$], and ZnCl$_2$ were used as received from Aldrich; azidotrimethylsilane was distilled prior to use. [FeCl$_2$(THF)$_{1.5}$],[27] [Pd(COD)Cl$_2$],[28] ethylene glycolditosylate,[29] TL^{tBu},[21a] [(BL^{Me})ZnCl$_2$] (**11**),[4d] and [(BL^{iPr})ZnCl$_2$] (**12**)[3e] were prepared according to literature procedures.

Dedicated Cluster

© 2015 WILEY-VCH Verlag GmbH & Co. KGaA, Weinheim

Gel Permeation Chromatography: The molecular weight and molecular weight distribution of the isolated polylactide samples were determined by gel permeation chromatography (GPC) in THF as mobile phase at a flow rate of 1 mL·min^{-1}. A combination of PSS SDV columns with porosities of 105 Å and 103 Å was used together with a HPLC pump (L6200, Merck Hitachi) and a refractive index detector (Smartline RI Detector 2300, Knauer) detector. Universal calibration was applied to evaluate the chromatographic results. Kuhn-Mark-Houwink (KMH) parameters for the polystyrene standards (K_{PS} = 0.011 ml/g, α_{PS} = 0.725) were taken from the literature [J. E. Mark, *Polymer Data Handbook*, Oxford University Press, New York, USA, **1999**]. Previous GPC measurements utilizing online viscosimetry detection revealed the KMH parameters for polylactide (K_{PLA} = 0.053 ml/g, α_{PLA} = 0.610).[19b]

***N*-Methyl-*N*′-(2,6-diisopropylphenyl)thiourea (1):** Methyl isothiocyanate (1.0 g, 13.7 mmol) was dissolved in acetonitrile (15 mL). 2,6-Diisopropylaniline was added dropwise to the solution under ambient conditions, and the mixture was stirred for 4 d. The solvent was evaporated, and the residue was recrystallized from toluene. The solid was isolated and washed with *n*-hexane (20 mL). The white product was isolated after drying in vacuo (1.20 g, 35 %). **^{1}H NMR** (200 MHz, $CDCl_3$): δ = 7.46 (s br, 1 H, N*H*Dipp), 7.43–7.16 (m, 3 H, *m*-,*p*-C*H*), 5.32 (d br, 1 H, N*H*Me), 3.14 (sept, 2 H, C*H*Me), 3.08 (d, 3 H, NCH_3), 1.18 (2 x d, 12 H, CHCH_3) ppm. **^{13}C NMR** (50.26 MHz, $CDCl_3$): δ = 182.5 (N*C*S), 147.8 (*o*-*C*), 132.3 (*i*-*C*) 129.9 (*p*-*C*), 124.6 (*m*-*C*), 31.9 (N*C*H$_3$), 28.5 (*C*HMe), 24.4 (CH*C*H$_3$), 23.3 (CH*C*H$_3$) ppm. **MS** (EI, 70 eV): *m*/*z* = 250 (M^+), 207 (M^+-C_3H_7). $C_{14}H_{22}N_2S$ (250.4): calcd. C 67.15, H 8.86, N 11.19 %; found C 66.91, H 8.35, N 11.07 %.

***N*-Methyl-*N*′-(2,6-diisopropylphenyl)imidazolin-2-thione (2):** **1** (5.19 g, 20.73 mmol) and 3-hydroxybutanone (1.83 g, 20.73 mmol) were dissolved in 1-hexanol (150 mL) and heated under reflux for 3 d. The solvent was evaporated and the residue was washed with small amounts of THF and then *n*-hexane. The remaining solid was dried in vacuo to afford the product as a white solid (4.06 g, 65 %). **^{1}H NMR** (300 MHz, C_6D_6): δ = 7.26 (m, 1 H, *p*-C*H*), 7.14 (m, 2 H, *m*-C*H*), 3.19 (s, 3 H, NCH_3), 2.74 (sept, 2 H, C*H*Me), 1.44 (m, 12 H, CHCH_3), 1.08 (s, 3 H, CCH_3), 1.06 (s, 3 H, CCH_3) ppm. **^{13}C NMR** (75.4 MHz, C_6D_6): δ = 165.3 (N*C*S), 147.1 (*o*-*C*), 132.7 (*i*-C), 129.7 (*p*-C), 124.1 (*m*-C), 120.4 (*C*Me), 120.2 (*C*Me), 31.3 (N*C*H$_3$), 28.8 (*C*HMe), 24.4 (CH*C*H$_3$), 23.5 (CH*C*H$_3$), 9.1 (C*C*H$_3$), 8.7 (C*C*H$_3$) ppm. $C_{18}H_{26}N_2S$ (302.5): calcd. C 71.48, H 8.66, N 9.26 %; found C 71.23, H 8.74, N 9.31 %.

1-(2,6-Diisopropylphenyl)-3,4,5-trimethylimidazolin-2-ylidene (3): Potassium (2.39 g, 61.2 mmol) was added to a solution of thione **2** (8.42 g, 27.8 mmol) in THF (150 mL) at room temperature, and the reaction mixture was heated under reflux overnight. The resulting suspension was filtered through Celite and washed with THF (3 × 20 mL). The solvent was evaporated and the residue was sublimed at 120 °C and 0.02 mbar to give a white crystalline solid (6.93 g, 92 %). **^{1}H NMR** (200 MHz, C_6D_6): δ = 7.30 (m, 2 H, *p*-C*H*), 7.19 (d, 1 H, *m*-C*H*), 3.45 (s, 3 H, NCH_3), 2.83 (2 H, sept, C*H*Me), 1.68 (m, 3 H, CCH_3), 1.62 (m, 3 H, CCH_3), 1.27 (d, 6 H, CHCH_3), 1.11 (d, 6 H, CHCH_3) ppm. **^{13}C NMR** (50.26 MHz, C_6D_6): δ = 215.3 (N*C*N), 146.9 (*o*-*C*), 137.6 (*i*-*C*), 128.8 (*p*-*C*), 123.7 (*m*-*C*), 124.2 (*C*Me), 122.5 (*C*Me), 35.7 (N*C*H$_3$), 28.5 (*C*HMe), 25.1 (CH*C*H$_3$), 23.1 (CH*C*H$_3$), 9.5 (C*C*H$_3$), 9.0 (C*C*H$_3$) ppm. **MS** (EI, 70 eV): *m*/*z* 357 (47) [M^+], 342 (100) [M+ – CH3], 285 (31) [M+ – TMS], 270 (71) [M+ – TMS-CH3]. $C_{18}H_{26}N_2$ (270.4): calcd. C 79.95, H 9.69, N 10.36 %; found C 79.99, H 9.57, N 10.05 %.

1-(2,6-Diisopropylphenyl)-3,4,5-trimethyl-2-(trimethylsilyl)iminoimidazoline (IPrNSiMe$_3$): The carbene **3** (1.74 g, 6.42 mmol) was dissolved in toluene (40 mL) and azidotrimethylsilane (1.28 mL, 1.11 g, 9.63 mmol) was added dropwise at room temperature. After complete addition, the reaction mixture was heated under reflux for 24 h. The mixture was filtered and the solvent evaporated. Sublimation at 150 °C and 0.04 mbar afforded the product as a pale yellow solid (1.81 g, 79 %). **^{1}H NMR** (200 MHz, C_6D_6): δ = 7.19 (m, 2 H, *p*-C*H*), 7.14 (d, 1 H, *m*-C*H*), 2.94 (sept, 2 H, C*H*Me), 2.82 (s, 3 H, NCH_3), 1.59 (s, 3 H, CCH_3), 1.49 (s, 3 H, CCH_3), 1.31 (d, 6 H, CHCH_3), 1.08 (d, 6 H, CHCH_3), 0.22 (s, 9 H, SiCH_3) ppm. **^{13}C NMR** (50.26 MHz, C_6D_6): δ = 148.5 (*o*-*C*), 143.9 (N*C*N), 133.7 (*i*-*C*), 129.3 (*p*-*C*), 123.9 (*m*-*C*), 114.4 (*C*Me), 113.9 (*C*Me), 28.7 (NCH$_3$), 28.4 (*C*HCH$_3$), 24.5 (CH*C*H$_3$), 23.8 (CH*C*H$_3$), 9.5 (C*C*H$_3$), 9.1 (C*C*H$_3$), 4.4 (Si*C*H$_3$). **MS** (EI, 70 eV): *m*/*z* 357 (47) [M^+], 342 (100) [M^+ – CH_3], 285 (31) [M^+ – TMS], 270 (71) [M^+ – TMS – CH_3]. $C_{21}H_{35}N_3Si$ (357.6): calcd. C 70.53, H 9.86, N 11.75 %; found C 69.87, H 9.60, N, 11.59 %.

1-(2,6-Diisopropylphenyl)-3,4,5-trimethylimidazolin-2-imine (4): 1-(2,6-Diisopropylphenyl)-3,4,5-trimethyl-2-(trimethylsilyl)iminoimidazoline (see previous protocol, 1.81 g, 5.07 mmol) was dissolved in methanol (20 mL) and stirred for 24 h at ambient temperature. All volatiles were removed under vacuum. The residue was recrystallized from THF and isolated by filtration. After drying in vacuo, the product was obtained as a white solid (1.45 g, 79 %). **^{1}H NMR** (200 MHz, C_6D_6): δ = 7.22 (m, 1 H, *p*-C*H*), 7.10 (m, 2 H, *m*-C*H*), 4.39 (s br, 1 H, N*H*), 3.44 (s, 3 H, NCH_3), 2.90 (sept, 2 H, C*H*Me), 1.52 (s, 3 H, CCH_3), 1.45 (s, 3 H, CCH_3), 1.19 (d, 6 H, CHCH_3), 1.05 (d, 6 H, CHCH_3) ppm. **^{13}C NMR** (50.26 MHz, C_6D_6): δ = 155.7 (N*C*N), 150.0 (*o*-C), 131.4 (*i*-*C*), 130.5 (*p*-*C*), 125.1 (*m*-*C*) 115.8 (*C*Me), 114.3 (*C*Me), 29.2 (*C*HCH$_3$), 28.9 (NCH$_3$), 25.2 (CH*C*H$_3$), 24.1 (CH*C*H$_3$), 9.5 (C*C*H$_3$), 9.1 (C*C*H$_3$) ppm. **MS** (EI, 70 eV): *m*/*z* = 285 (39) [M^+], 270 (100) [M^+ – CH_3]. $C_{18}H_{27}N_3$ (285.4): calcd. C 75.74, H 9.53, N 14.72 %; found C 75.49, H 9.50, N 14.04 %.

1,2-Bis(1-(2,6-diisopropylphenyl)-3,4,5-trimethylimidazolin-2-imino)ethylene (5, BL^{Dipp,Me}): Ethylene glycolditosylate (0.94 g, 2.54 mmol) and the imine **4** (1.45 g, 5.08 mmol) were dissolved in toluene (70 mL) and stirred for 72 h at 115 °C. Afterwards, the solvent was evaporated, and the residue was washed with *n*-hexane (2 × 20 mL) and diethyl ether (20 mL). The remaining solid (2.09 g, 2.22 mmol) was suspended in THF (60 mL) and KO*t*Bu (597.9 mg, 5.33 mmol) was added. The mixture was stirred overnight at ambient temperature, filtered and washed with THF (2 × 10 mL). The solvent was removed and the remaining solid was dried in vacuo to yield the product as a pale yellow solid (1.31 g, 98 %). **^{1}H NMR** (300 MHz, C_6D_6): δ = 7.11–7.06 (m, 2 H, *p*-C*H*), 6.95–6.93 (m, 4 H, *m*-C*H*), 3.09 (s, 4 H, CH_2), 3.04 (sept, 4 H, C*H*Me), 2.85 (s, 6 H, NCH_3), 1.46 (s, 6 H, CCH_3), 1.34 (s, 6 H, CCH_3), 1.18 (d, 12 H, CHCH_3), 0.99 (d, 12 H, CHCH_3) ppm. **^{13}C NMR** (75.48 MHz, C_6D_6): δ = 148.2 (*o*-*C*), 145.0 (N*C*N), 134.8 (*i*-*C*), 128.7 (*p*-*C*), 123.3 (*m*-*C*), 114.8 (*C*Me), 113.4 (*C*Me), 50.9 (*C*H$_2$), 28.3 (NCH$_3$), 28.2 (CH*C*H$_3$), 24.0 (CH*C*H$_3$), 23.6 (*C*HCH$_3$), 8.9 (C*C*H$_3$), 8.7 (C*C*H$_3$) ppm. **MS** (EI, 70 eV): *m*/*z* = 596 (M^+), 298 (M^+/2). $C_{38}H_{56}N_6$ (596.9): calcd. C 76.46, H 9.46, N 14.08 %; found C 75.62, H 9.25, N 13.65 %.

[(BL^{Dipp,Me})FeCl$_2$] (6): A THF solution (10 mL) of BL^{Dipp,Me} (142.1 mg, 0.24 mmol) was added dropwise at ambient temperature to a solution of [$FeCl_2(THF)_{1.5}$] (50.0 mg, 0.23 mmol) in THF (15 mL) and stirred overnight. The volume of the solution was reduced to 5 mL, and the product was fully precipitated by addition of *n*-hexane (30 mL). Filtration, washing with *n*-hexane (2 × 5 mL), and drying in vacuo afforded the product as a white solid (107.6 mg, 63 %). **MS** (EI, 70 eV): *m*/*z* = 722 (M^+), 298 (BL^{Dipp,Me}/2). $C_{38}H_{56}N_6Cl_2Fe$ (723.7): calcd. C 63.07, H 7.80, N 11.61 %; found C 62.74, H 7.53, N 11.34 %.

Dedicated Cluster

© 2015 WILEY-VCH Verlag GmbH & Co. KGaA, Weinheim

[(BL^{Dipp,Me})NiCl$_2$] (7): BL^{Dipp,Me} (100.0 mg, 0.17 mmol) in THF (5 mL) was added to a suspension of [(DME)NiCl$_2$] (36.0 mg, 0.16 mmol) in THF (10 mL) at ambient temperature. The mixture was stirred overnight, and the volume was reduced to 5 mL. The product was precipitated with *n*-hexane (30 mL), filtered off, washed with *n*-hexane (2 × 5 mL) and dried in vacuo. The product was isolated as a red solid (95.3 mg, 80 %). **MS** (EI, 70 eV): *m*/*z* = 726 (M$^+$), 298 (BL^{Dipp,Me}/2). $C_{38}H_{56}N_6Cl_2Ni$ (726.5): calcd. C 62.82, H 7.77, N 11.57 %; found C 60.87, H 7.54, N 10.83 %.

[(BL^{Dipp,Me})ZnCl$_2$] (8): A solution of BL^{Dipp,Me} (89.5 mg, 0.15 mmol) in acetonitrile (5 mL) was added to a suspension of $ZnCl_2$ (20.0 mg, 0.15 mmol) in acetonitrile (10 mL) at ambient temperature and stirred for 72 h. The volume was reduced to 5 mL and the product precipitated by addition of diethyl ether (30 mL). Filtration, washing with diethyl ether (2 × 10 mL) and drying in vacuo afforded the colorless product (107.4 mg, 97 %). **^{1}H NMR** (400 MHz, $CDCl_3$): δ = 7.32 (t, 2 H, *p*-C*H*), 7.09 (d, 4 H, *m*-C*H*), 3.61 (s, 6 H, NCH_3), 2.73 (sept, 4 H, C*H*Me), 2.39 (s, 4 H, CH_2), 2.04 (s, 6 H, CCH_3), 1.56 (s, 6 H, CCH_3), 1.08 (2 x d, 24 H, CHCH_3) ppm. **^{13}C NMR** (50.26 MHz, $CDCl_3$): δ = 149.7 (N*C*N), 147.5 (*o*-*C*), 132.5 (*i*-*C*), 129.7 (*p*-*C*), 123.7 (*m*-*C*), 117.6 (*C*Me), 116.4 (*C*Me), 47.4 (*C*H$_2$), 31.6 (N*C*H$_3$), 28.0 (*C*HCH$_3$), 24.3 (CH*C*H$_3$), 23.6 (CH*C*H$_3$), 9.5 (C*C*H$_3$), 8.8 (C*C*H$_3$) ppm. **MS** (EI, 70 eV): *m*/*z* = 733 (M$^+$), 298 (BL^{Dipp,Me}/2). $C_{38}H_{56}N_6Cl_2Zn$ (733.2): calcd. C 62.25, H 7.70, N 11.46 %; found C 62.22, H 7.78, N 10.49 %.

[(BL^{Dipp,Me})PdCl$_2$] (9): A solution of BL^{Dipp,Me} (210 mg, 0.35 mmol) in THF (15 mL) was added to a suspension of [(COD)PdCl$_2$] (100 mg, 0.35 mmol) in THF (2 mL). A red solution formed instantaneously. After stirring overnight, the product was precipitated by addition of hexane, isolated by filtration, washed with hexane (3 × 5 mL), and dried in vacuo. The product was isolated as a red solid (260 mg, 96 %). **^{1}H NMR** (300 MHz, CD_2Cl_2): δ = 7.41 (m, 2 H, *p*-C*H*), 7.23 (m, 4 H, *m*-C*H*), 3.77 (br. m, 6 H, NCH_3), 3.50–2.00 (m, 8 H, C*H*Me and CH_2), 2.05 (m, 6 H, CCH_3), 1.62 (s, 6 H, CCH_3), 1.07 (br. m, 12 H CHCH_3) ppm. **^{13}C NMR** (75 MHz, CD_2Cl_2): δ = 152.9 (NCN), 148.6 (*o*-*C*), 131.6 (*i*-*C*), 130.3 (*p*-*C*), 124.7 (*m*-*C*), 119.3 (*C*Me), 118.6 (s, *C*Me), 32.7 (N*C*H$_3$), 28.2 (*C*HMe), 24.7 (CH*C*H$_3$), 24.4 (CH*C*H$_3$), 9.5 (C*C*H$_3$), 9.1 (s, C*C*H$_3$) ppm. $C_{38}H_{56}Cl_2N_6Pd$ (774.2): calcd. C 58.95, H 7.29, N 10.85 %; found C 58.92, H 7.17, N 11.84 %.

[(TL^{tBu})ZnCl$_2$] (10): A solution of TL^{tBu} (200 mg, 0.405 mmol) in THF (10 mL) was added dropwise to a solution of $ZnCl_2$ (55.22 mg, 0.98 mmol) in THF (10 mL) at room temperature. During the addition of the ligand, the formation of a pale yellow precipitate was observed. The suspension was stirred for 12 h followed by reduction of THF volume to 10 mL. The product was fully precipitated by addition of *n*-hexane (20 mL). Filtration, washing with *n*-hexane (2 × 10 mL) and drying in vacuo afforded the product as a pale yellow solid (254 mg, 99 %). **^{1}H NMR** (200 MHz, $CDCl_3$): δ = 7.83 (t, 1 H, *p*-Py), 7.59 (d, 2 H, *m*-Py), 6.59 (s, 4 H, NC*H*), 4.98 (s, 4 H, CH_2), 1.66 (s, 36 H, CH_3) ppm. **^{13}C NMR** (50 MHz, $CDCl_3$): δ = 161.3 (*o*-*C*), 150.5 (N*C*N), 138.9 (*p*-*C*), 119.8 (*m*-*C*), 111.1 (N*C*H), 67.9 (*C*H$_2$), 57.5 (N*C*Me), 30.3 (C*C*H$_3$) ppm. $C_{29}H_{47}N_7Cl_2Zn$ (630.0): calcd. C 55.28, H 7.52, N 15.56 %; found C 55.17, H 7.71, N 13.84 %.

General Procedure for D,L-Lactide Polymerization with Zinc Complexes: D,L-Lactide (3.603 g, 25 mmol) and the initiator (I/M ratio 1/500) were weighed into a 50 mL flask, which was closed with a glass stopper. The D,L-lactide was used as purchased from Purac without further purification steps. The reaction vessel was heated at 150 °C. After the reaction time of 24 or 48 h the polymer melt was allowed to cool to room temperature and then dissolved in 25 mL of dichloromethane. The PLA was precipitated in 350 mL of ice-cooled ethanol und dried under vacuum at 50 °C.

X-ray Diffraction Analyses: Data are summarized in Table 4. Crystals were mounted in inert oil on glass fibres. Data were recorded at 100 K with an Oxford Diffraction diffractometers using monochromated Mo-K_α or mirror-focused Cu-K_α radiation. Absorption corrections were performed on the basis of multi-scans. Structures were refined anisotropically on F^2 using the program SHELXL-97.[30] Hydrogen atoms were included using rigid idealized methyl groups or a riding model. *Exceptions and special features*: The two independent molecules of compound **3** are related to a good approximation by the translation **c**/2, but the different orientations of several groups (notably the isopropyl

Dedicated Cluster

Table 4. Crystallographic data.

	2	**3**	**4**	**5**	6·THF	**7**·1.5THF	**8**·CH_2Cl_2	**9**·CH_3CN	**10**·2.5 THF	**10**·HCl·CH_2Cl_2
Empirical formula	$C_{18}H_{26}N_2S$	$C_{18}H_{26}N_2$	$C_{18}H_{27}N_3$	$C_{38}H_{56}N_6$	$C_{42}H_{64}Cl_2FeN_6O$	$C_{44}H_{68}Cl_2N_6NiO_{1.5}$	$C_{39}H_{58}Cl_4N_6Zn$	$C_{40}H_{59}Cl_2N_7Pd$	$C_{39}H_{67}Cl_2N_7ZnO_{2.5}$	$C_{30}H_{50}Cl_5N_7Zn$
a /Å	12.3432(8)	22.3995(6)	12.5623(10)	13.8023(12)	18.1232(4)	10.9767(6)	9.4516(6)	10.6162(2)	9.9010(10)	9.1131(10)
b /Å	9.2267(6)	6.6797(4)	8.8476(6)	15.0429(14)	14.4546(4)	18.7461(12)	15.5494(4)	14.7074(5)	13.2950(12)	14.1319(14)
c /Å	15.3639(8)	23.0171(8)	15.1410(14)	18.4481(18)	17.5963(6)	23.3544(16)	14.6054(4)	15.2574(6)	32.069(3)	14.6013(14)
α /°	90	90	90	88.386(8)	90	69.943(6)	90	116.578(4)	90	89.791(8)
β /°	98.086(6)	103.730(4)	97.140(8)	70.584(8)	112.349(4)	80.878(6)	91.985(4)	94.798(3)	91.282(10)	84.212(8)
γ /°	90	90	90	76.085(8)	90	85.304(6)	90	101.245(3)	90	82.792(8)
V /Å^3	1732.35(18)	3345.5(2)	1669.8(2)	3500.9(6)	4263.3(2)	4455.2(5)	2145.22(16)	2049.55(11)	4220.3(7)	1856.0(3)
Z	4	8	4	4	4	4	2	2	4	2
Formula weight	302.47	270.41	285.43	596.89	795.74	834.65	818.08	815.24	810.27	751.39
Space group	$P2_1/c$	$P2_1/n$	$P2_1/c$	$P\bar{1}$	Cc	$P\bar{1}$	$P2_1$	$P\bar{1}$	$P2_1/c$	$P\bar{1}$
T /K	100(2)	100(2)	100(2)	100(2)	100(2)	100(2)	100(2)	100(2)	100(2)	100(2)
λ /Å	0.71073	0.71073	0.71073	0.71073	0.71073	0.71073	0.71073	0.71073	1.54184	1.54184
$D_{calcd.}$ /g·cm^{-3}	1.160	1.074	1.135	1.132	1.240	1.244	1.267	1.321	1.275	1.345
μ /mm^{-1}	0.183	0.063	0.068	0.067	0.518	0.596	0.855	0.620	2.302	4.465
Reflection collected	43466	86259	25757	68675	42068	128780	56112	142675	57156	30927
Independent reflections	4296, R_{int} = 0.0365	9360, R_{int} = 0.0444	2950, R_{int} = 0.0822	14259, R_{int} = 0.0721	10571, R_{int} = 0.0443	23857, R_{int} = 0.0420	10667, R_{int} = 0.0209	12207, R_{int} = 0.0409	7994, R_{int} = 0.1162	7661, R_{int} = 0.0662
Goodness of fit on F^2	1.049	1.082	0.813	0.835	0.930	0.912	1.022	1.051	0.893	1.045
$R(F_o)$, $[I > 2\sigma(I)]$	0.0371	0.0468	0.0368	0.0417	0.0318	0.0317	0.0174	0.0259	0.0518	0.0431
$R_w(F_o^2)$	0.1026	0.1255	0.0688	0.0678	0.0643	0.0785	0.0448	0.0594	0.1190	0.1070
$\Delta\rho$ /e·Å^{-3}	0.395/–0.267	0.446/–0.338	0.139/–0.202	0.184/–0.177	0.323/–0.359	0.381/–0.248	0.398/–0.302	0.482/–0.536	0.505/–0.458	0.662/–0.482

© 2015 WILEY-VCH Verlag GmbH & Co. KGaA, Weinheim

group at C13–15) show that this translation symmetry is not exact. The NH hydrogen atoms of compounds **4** and **10**·HCl·CH_2Cl_2 were refined freely. Compound **6** crystallizes in the non-centrosymmetric space group *Cc*, but the symmetry is close to *C*2/*c* (the complex displays twofold symmetry within an r.m.s.d. of 0.09 Å). Nevertheless, the poor refinement in the higher symmetry space group (some high *U* values, high wR_2 of 0.30) convinces us that *Cc* is correct. The structure was refined as an enantiomeric twin with relative component volumes 0.51, 0.49(1). Compound **7** crystallizes with 3THF in the asymmetric unit; two were refined satisfactorily, but the third had to be removed mathematically using the routine SQUEEZE (SQUEEZE forms part of the PLATON program package: A. L. Spek, University of Utrecht, Netherlands). Similarly, compound **10** crystallized with 2.5THF in the asymmetric unit, of which 1.5 were removed with SQUEEZE. The dichloromethane solvent molecule of **10**·HCl·CH_2Cl_2 is disordered, but was refined satisfactorily. Compound **8** crystallizes only by chance in the Sohncke space group $P2_1$; the Flack parameter refined to –0.003(3). The carbon atoms of the chelate ring in compound **9** are disordered over two positions, although one position predominates; suitable restraints were employed to improve refinement stability, but dimensions of disordered groups should always be interpreted with caution.

Crystallographic data (excluding structure factors) for the structures in this paper have been deposited with the Cambridge Crystallographic Data Centre, CCDC, 12 Union Road, Cambridge CB21EZ, UK. Copies of the data can be obtained free of charge on quoting the depository numbers CCDC-1409537 (**2**), CCDC-1409538 (**3**), CCDC-1409539 (**5**), CCDC-1409540 (**4**), CCDC-1409541 (**6**·THF), CCDC-1409542 (**7**·1.5THF), CCDC-1409543 (**8**·CH_2Cl_2), CCDC-1409544 (**10**·2.5THF), CCDC-1409545 (**10**·HCl·CH_2Cl_2), CCDC-1409546 (**9**·CH_3CN), CCDC-1409547 (**5**·2HCl·3CH_2Cl_2), and CCDC-1409548 ([Rh(COD)(**5**)]BF_4·3THF (Fax: +44-1223-336-033; E-Mail: deposit@ccdc.cam.ac.uk, http://www.ccdc.cam.ac.uk).

Supporting Information (see footnote on the first page of this article): Further X-ray structure determinations of **5**·2HCl·3CH_2Cl_2) and [Rh(COD)(**5**)]BF_4·3THF; selected NMR spectra.

Acknowledgements

We thank *Dr. Cristian G. Hrib*, *Dr. Constantin G. Daniliuc*, and Mr. *Dirk Bockfeld* (M.Sc.) for X-ray crystallographic support. S. H.-P. thanks *Prof. Klaus Huber* for GPC measurements.

References

[1] X. Wu, M. Tamm, *Coord. Chem. Rev.* **2014**, *260*, 116–138.
[2] a) O. Bienemann, A. Hoffmann, S. Herres-Pawlis, *Rev. Inorg. Chem.* **2011**, *33*, 83–108; b) I. dos Santos Vieira, S. Herres-Pawlis, *Eur. J. Inorg. Chem.* **2012**, 765–774; c) H.-J. Himmel, *Z. Anorg. Allg. Chem.* **2013**, *639*, 1940–1952; d) J. Sundermeyer, V. Raab, E. Gaoutchenova, U. Garrelts, N. Abacilar, K. Harms, in: *Activating Unreactive Substrates*, Wiley-VCH Verlag, Weinheim, **2009**; e) S. Herres-Pawlis, *Nachr. Chem.* **2009**, *57*, 20–23; f) N. Kuhn, M. Göhner, M. Grathwohl, J. Wiethoff, G. Frenking, Y. Chen, *Z. Anorg. Allg. Chem.* **2003**, *629*, 793–802.
[3] a) D. Petrovic, T. Glöge, T. Bannenberg, C. G. Hrib, S. Randoll, P. G. Jones, M. Tamm, *Eur. J. Inorg. Chem.* **2007**, 3472–3475; b) D. Petrovic, C. G. Hrib, S. Randoll, P. G. Jones, M. Tamm, *Organometallics* **2008**, *27*, 778–783; c) T. K. Panda, C. G. Hrib, P. G. Jones, J. Jenter, P. W. Roesky, M. Tamm, *Eur. J. Inorg. Chem.* **2008**, 4270–4279; d) T. Glöge, D. Petrovic, C. G. Hrib, P. G. Jones, M. Tamm, *Z. Naturforsch.* **2008**, *63b*, 1155–1159; e) T. Glöge, D. Petrovic, C. G. Hrib, C. Daniliuc, E. Herdtweck, P. G. Jones, M. Tamm, *Z. Anorg. Allg. Chem.* **2010**, *636*, 2303–2308; f) J. Bogojeski, R. Jelić, D. Petrović, E. Herdtweck, P. G. Jones, M. Tamm, Ž. D. Bugarčić, *Dalton Trans.* **2011**, *40*, 6515–6523.
[4] a) D. Petrovic, L. M. R. Hill, P. G. Jones, W. B. Tolman, M. Tamm, *Dalton Trans.* **2008**, 887–894; b) S. Randoll, P. G. Jones, M. Tamm, *Organometallics* **2008**, *27*, 3232–3239; c) T. Glöge, D. Petrovic, C. Hrib, P. G. Jones, M. Tamm, *Eur. J. Inorg. Chem.* **2009**, 4538–4546; d) J. Börner, U. Flörke, T. Glöge, T. Bannenberg, M. Tamm, M. D. Jones, A. Döring, D. Kuckling, S. Herres-Pawlis, *J. Mol. Catal. A* **2010**, *316*, 139–145; e) S.-A. Filimon, C. G. Hrib, S. Randoll, I. Neda, P. G. Jones, M. Tamm, *Z. Anorg. Allg. Chem.* **2010**, *636*, 691–699; f) J. Volbeda, P. G. Jones, M. Tamm, *Inorg. Chim. Acta* **2014**, *422*, 158–166; g) T. Glöge, K. Jess, T. Bannenberg, P. G. Jones, N. Langenscheidt-Dabringhausen, A. Salzer, M. Tamm, *Dalton Trans.* **2015**, *44*, 11717–11724.
[5] M. Tamm, D. Petrovic, S. Randoll, S. Beer, T. Bannenberg, P. G. Jones, J. Grunenberg, *Org. Biomol. Chem.* **2007**, *5*, 523–530.
[6] a) K. E. Allen, J. Campos, O. Daugulis, M. Brookhart, *ACS Catal.* **2015**, *5*, 456–464; b) T. Vaidya, K. Klimovica, A. M. LaPointe, I. Keresztes, E. B. Lobkovsky, O. Daugulis, G. W. Coates, *J. Am. Chem. Soc.* **2014**, *136*, 7213–7216; c) D. Zhang, E. T. Nadres, M. Brookhart, O. Daugulis, *Organometallics* **2013**, *32*, 5136–5143; d) L. K. Johnson, C. M. Killian, M. Brookhart, *J. Am. Chem. Soc.* **1995**, *117*, 6414–6415.
[7] a) F. E. Hahn, *Angew. Chem. Int. Ed.* **2006**, *45*, 1348–1352; b) F. E. Hahn, M. C. Jahnke, *Angew. Chem. Int. Ed.* **2008**, *47*, 3122–3172; c) M. Jahnke, F. E. Hahn, in *Topics in Organometallic Chemistry* (Eds.: R. Chauvin, Y. Canac), Springer Berlin Heidelberg, **2010**; d) M. N. Hopkinson, C. Richter, M. Schedler, F. Glorius, *Nature* **2014**, *510*, 485–496; e) W. A. Herrmann, C. Köcher, *Angew. Chem. Int. Ed. Engl.* **1997**, *36*, 2162–2187.
[8] a) T. Bernardi, S. Badel, P. Mayer, J. Groelly, P. de Frémont, B. Jacques, P. Braunstein, M.-L. Teyssot, C. Gaulier, F. Cisnetti, A. Gautier, S. Roland, *ChemMedChem* **2014**, *9*, 1140–1144; b) D. Brissy, M. Skander, P. Retailleau, G. Frison, A. Marinetti, *Organometallics* **2009**, *28*, 140–151; c) C. Cesari, S. Conti, S. Zacchini, V. Zanotti, M. C. Cassani, R. Mazzoni, *Dalton Trans.* **2014**, *43*, 17240–17243; d) B. R. Dible, M. S. Sigman, *Inorg. Chem.* **2006**, *45*, 8430–8441; e) A. Flahaut, S. Roland, P. Mangeney, *J. Organomet. Chem.* **2007**, *692*, 5754–5762; f) J. Li, J. Peng, Y. Bai, G. Lai, X. Li, *J. Organomet. Chem.* **2011**, *696*, 2116–2121; g) K. H. Park, S. Y. Kim, S. U. Son, Y. K. Chung, *Eur. J. Org. Chem.* **2003**, *2003*, 4341–4345; h) S. Roland, W. Cotet, P. Mangeney, *Eur. J. Inorg. Chem.* **2009**, *2009*, 1796–1805; i) G. Venkatachalam, M. Heckenroth, A. Neels, M. Albrecht, *Helv. Chim. Acta* **2009**, *92*, 1034–1045.
[9] W. Walter, K.-P. Rueß, *Justus Liebigs Ann. Chem.* **1974**, 225–242.
[10] N. Kuhn, T. Kratz, *Synthesis* **1993**, 561–562.
[11] a) N. Burford, A. D. Phillips, H. A. Spinney, K. N. Robertson, T. S. Cameron, R. McDonald, *Inorg. Chem.* **2003**, *42*, 4949–4954; b) N. Kuhn, J. Fahl, R. Fawzi, M. Steimann, *Z. Kristallogr. New Cryst. Struct.* **1998**, *213*, 434–435; c) J. Pesch, K. Harms, T. Bach, *Eur. J. Org. Chem.* **2004**, *2004*, 2025–2035.
[12] a) A. A. Danopoulos, S. Winston, T. Gelbrich, M. B. Hursthouse, R. P. Tooze, *Chem. Commun.* **2002**, 482–483; b) X. Hu, I. Castro-Rodriguez, K. Meyer, *Organometallics* **2003**, *22*, 3016–3018; c) M. Nonnenmacher, D. Kunz, F. Rominger, T. Oeser, *Chem. Commun.* **2006**, 1378–1380; d) J. A. Wright, A. A. Danopoulos, W. B. Motherwell, R. J. Carroll, S. Ellwood, J. Saßmannshausen, *Eur. J. Inorg. Chem.* **2006**, *2006*, 4857–4865.
[13] a) A. J. Arduengo, R. L. Harlow, M. Kline, *J. Am. Chem. Soc.* **1991**, *113*, 361–363; b) A. J. Arduengo, H. V. R. Dias, R. L. Harlow, M. Kline, *J. Am. Chem. Soc.* **1992**, *114*, 5530–5534; c) A. J. Arduengo, H. V. R. Dias, D. A. Dixon, R. L. Harlow, W. T. Klooster, T. F. Koetzle, *J. Am. Chem. Soc.* **1994**, *116*, 6812–6822.
[14] H. Staudinger, J. Meyer, *Helv. Chim. Acta* **1919**, *2*, 635–646.

 © 2015 WILEY-VCH Verlag GmbH & Co. KGaA, Weinheim

[15] J. March, *Advanced Organic Chemistry*, John Wiley & Sons, New York, **1992**.
[16] a) A. Bondi, *J. Phys. Chem.* **1964**, *68*, 441–451; b) R. S. Rowland, R. Taylor, *J. Phys. Chem.* **1996**, *100*, 7384–7391.
[17] a) A. Neuba, R. Haase, M. Bernard, U. Flörke, S. Herres-Pawlis, *Z. Anorg. Allg. Chem.* **2008**, *634*, 2511–2517; b) J. Börner, U. Flörke, K. Huber, A. Döring, D. Kuckling, S. Herres-Pawlis, *Chem. Eur. J.* **2009**, *15*, 2362–2376.
[18] L. Yang, D. R. Powell, R. P. Houser, *Dalton Trans.* **2007**, 955–964; this four-coordinate arrangement index τ_4 is related to the five-coordinate arrangement index $\tau_5 = (\alpha - \beta)/60°$, which was developed for describing distortions between trigonal-bipyramidal ($\tau_5 = 1$) and square-pyramidal environments ($\tau_5 = 0$), see: A. W. Addison, T. N. Rao, J. Reedijk, J. van der Rijn, G. C. Verschoor, *J. Chem. Soc., Dalton Trans.* **1984**, 1349–1356.
[19] a) H. Wittmann, A. Schorm, J. Sundermeyer, *Z. Anorg. Allg. Chem.* **2000**, 626; b) J. Börner, S. Herres-Pawlis, U. Flörke, K. Huber, *Eur. J. Inorg. Chem.* **2007**, *2007*, 5645–5651; c) M. Reinmuth, U. Wild, D. Rudolf, E. Kaifer, M. Enders, H. Wadepohl, H.-J. Himmel, *Eur. J. Inorg. Chem.* **2009**, 4795–4808; d) A. Peters, C. Trumm, M. Reinmuth, D. Emeljanenko, E. Kaifer, H.-J. Himmel, *Eur. J. Inorg. Chem.* **2009**, 3791–3800; e) A. Neuba, S. Herres-Pawlis, O. Seewald, J. Börner, A. J. Heuwing, U. Flörke, G. Henkel, *Z. Anorg. Allg. Chem.* **2010**, *636*, 2641–2649; f) P. Roquette, C. König, O. Hübner, A. Wagner, E. Kaifer, M. Enders, H.-J. Himmel, *Eur. J. Inorg. Chem.* **2010**, 4770–4782; g) P. Roquette, A. Maronna, A. Peters, E. Kaifer, H.-J. Himmel, C. Hauf, V. Herz, E.-W. Scheidt, W. Scherer, *Chem. Eur. J.* **2010**, *16*, 1336–1350; h) P. Roquette, A. Maronna, M. Reinmuth, E. Kaifer, M. Enders, H.-J. Himmel, *Inorg. Chem.* **2011**, *50*, 1942–1955; i) U. Wild, E. Kaifer, H.-J. Himmel, *Eur. J. Inorg. Chem.* **2011**, 4220–4233; j) A. Maronna, O. Hübner, M. Enders, E. Kaifer, H.-J. Himmel, *Chem. Eur. J.* **2013**, *19*, 8958–8977; k) S. Wiesner, A. Ziesak, M. Reinmuth, P. Walter, E. Kaifer, H. Wadepohl, H.-J. Himmel, *Eur. J. Inorg. Chem.* **2013**, 163–171; l) E. Bindewald, R. Lorenz, O. Hübner, D. Brox, D.-P. Herten, E. Kaifer, H.-J. Himmel, *Dalton Trans.* **2015**, *44*, 3467–3485.
[20] a) N. Kuhn, M. Grathwohl, M. Steimann, G. Henkel, *Z. Naturforsch.* **1998**, *53b*, 997–1003; b) U. Wild, O. Hübner, A. Maronna, M. Enders, E. Kaifer, H. Wadepohl, H.-J. Himmel, *Eur. J. Inorg. Chem.* **2008**, 4440–4447.
[21] a) D. Petrovic, T. Bannenberg, S. Randoll, P. G. Jones, M. Tamm, *Dalton Trans.* **2007**, 2812–2822; b) T. K. Panda, D. Petrovic, T. Bannenberg, C. G. Hrib, P. G. Jones, M. Tamm, *Inorg. Chim. Acta* **2008**, *361*, 2236–2242; c) S.-A. Filimon, D. Petrovic, J. Volbeda, T. Bannenberg, P. G. Jones, C.-G. Freiherr von Richthofen, T. Glaser, M. Tamm, *Eur. J. Inorg. Chem.* **2014**, *2014*, 5997–6012.
[22] T. Steiner, *Angew. Chem. Int. Ed.* **2002**, *41*, 48–76.
[23] a) J. Börner, I. dos Santos Vieira, A. Pawlis, A. Döring, D. Kuckling, S. Herres-Pawlis, *Chem. Eur. J.* **2011**, *17*, 4507–4512; b) J. Börner, U. Flörke, A. Döring, D. Kuckling, M. D. Jones, M. Steiner, M. Breuning, S. Herres-Pawlis, *Inorg. Chem. Commun.* **2010**, *13*, 369–371.
[24] a) R. H. Platel, L. M. Hodgson, C. K. Williams, *Polym. Rev.* **2008**, *48*, 11–63; b) J. Wu, T.-L. Yu, C.-T. Chen, C.-C. Lin, *Coord. Chem. Rev.* **2006**, *250*, 602–626; c) B. J. O'Keefe, M. A. Hillmyer, W. B. Tolman, *J. Chem. Soc., Dalton Trans.* **2001**, 2215–2224; d) O. Dechy-Cabaret, B. Martin-Vaca, D. Bourissou, *Chem. Rev.* **2004**, *104*, 6147–6176; e) R. E. Drumright, P. R. Gruber, D. E. Henton, *Adv. Mater.* **2000**, *12*, 1841–1846.
[25] B. M. Chamberlain, M. Cheng, D. R. Moore, T. M. Ovitt, E. B. Lobkovsky, G. W. Coates, *J. Am. Chem. Soc.* **2001**, *123*, 3229–3238.
[26] S. Pracha, S. Praban, A. Niewpung, G. Kotpisan, P. Kongsaeree, S. Saithong, T. Khamnaen, P. Phiriyawirut, S. Charoenchaidet, K. Phomphrai, *Dalton Trans.* **2013**, *42*, 15191–15198.
[27] a) R. J. Kern, *J. Inorg. Nucl. Chem.* **1962**, *24*, 1105–1109; b) H. Zhao, R. Clérac, J.-S. Sun, X. Ouyang, J. M. Clemente-Juan, C. J. Gómez-García, E. Coronado, K. R. Dunbar, *J. Solid State Chem.* **2001**, *159*, 281–292.
[28] D. Drew, J. R. Doyle, A. G. Shaver, *Inorg. Synth.* **2007**, *28*, 346–349.
[29] M. Ouchi, Y. Inoue, Y. Liu, S. Nagamune, S. Nakamura, K. Wada, T. Hakushi, *Bull. Chem. Soc. Jpn.* **1990**, *63*, 1260–1262.
[30] G. M. Sheldrick, *Acta Crystallogr., Sect. A* **2008**, *64*, 112–122.

Received: July 2, 2015
Published Online: September 3, 2015

Dedicated Cluster

 © 2015 WILEY-VCH Verlag GmbH & Co. KGaA, Weinheim